JOURNAL OF THERMOPHYSICS AND HEAT TRANSFER
Vol. 12, No. 1, January–March 1998

Vaporization of Binary Fuel Mixture Droplets in a Thermal Wind Tunnel

A. Daïf,* M. Bouaziz,† and M. Grisenti‡
Université de Perpignan, Perpignan 66860, France

The authors present the study of vaporization, in forced convection, of two or three binary fuel mixture droplets. The droplets are situated one behind the other and are evaporated by forced convection in a thermal wind tunnel equipped with a video recording system. The image processing provides the radius regression of the droplets in accordance with the elapsed time, which is compared with results from a calculated model based on the concept of the gaseous film surrounding the droplets and the source of heat and mass transfer. During the period of suspension of the droplets, their vaporization begins in natural convection. From the opening of the obturator that allows the arrival of hot airflow, the forced convection sequence begins, as does the interaction between droplets. Average Nusselt and Sherwood numbers used for the calculation of gaseous film thicknesses surrounding droplets come from established correlations in natural and forced convection. In the case of interaction, these Nusselt and Sherwood numbers are corrected. The experiments and calculations that are undertaken for several mixtures of heptane and decane, and for several distances between the droplets, are in good agreement. Numerical results of the validated model are analyzed using a systematic parametric study.

Nomenclature

B_M = mass transfer number, $\Sigma_{j=1}^{2} (Y_{gjs} - Y_{gj\infty})/(1 - \Sigma_{j=1}^{2} Y_{gjs})$
B_T = heat transfer number, $Cp(T_\infty - T_s)/q_g$
Cp = specific heat at constant pressure, J kg^{-1} K^{-1}
D = mass diffusion coefficient, cm^2 s^{-1}
d_{ik} = separation distance between droplet $n°i$ and $n°k$, m
d'_{ik} = dimensionless separation distance, d_{ik}/r_{i0}
Gr_{Mj} = mass Grashof number of the j component, $g\beta_{Mj}[(Y_{gj\infty} - Y_{gjs})(2r_s)^3/\nu_\infty^2]$
Gr_m = average Grashof number, $(\nu_\infty^2/2\nu_f^2)(\Sigma_{j=1}^{2} Y_{lsj}Gr_{Mj} + Gr_T)$
Gr_T = thermal Grashof number, $g\beta_T[(T_\infty - T_s)(2r_s)^3/\nu_\infty^2]$
g = gravitational constant, m s^{-2}
K = average evaporation constant, $(1/N)\ \Sigma_{i=1}^{N} (\mathrm{d}r_i^2/\mathrm{d}t_i)$
M = molecular weight, kg mol^{-1}
$\overline{Nu}$ = average Nusselt number
Pr = Prandtl number, $\mu_f Cp_f/\lambda_f$
q = heat transferred into the droplet, J
Re = Reynolds number, $2r_{10}\rho_\infty U_\infty/\mu_\infty$
Re_m = average Reynolds number, $2r_s\rho_\infty U_\infty/\mu_f$
r = droplet radius, m
r_{fM} = limit of the integration area for mass transfer
r_{fT} = limit of the integration area for heat transfer
Sc = Schmidt number, $\mu_f/\rho_f D_{gf}$
$\overline{Sh}$ = average Sherwood number
T = temperature, K
t = time, s
Y = mass fraction
β_{Mj} = mass expansion coefficient of the j component, $M_{\mathrm{air}}/M_j - 1$
β_T = thermal expansion coefficient of the fluid, $1/T_\infty$, K^{-1}
λ = thermal conductivity, W m^{-1} K^{-1}
μ = dynamic viscosity, N s m^{-2}
ν = kinematic viscosity, m^2 s^{-1}
ρ = density, kg m^{-3}

Subscripts

cr = critical
f = film
g = gas
i, k = droplet index
iso = isolated
j = component index, 1, 2
ℓ = liquid
M = mass
s = surface
T = thermal
0 = initial
∞ = ambient gas

Superscript

$'$ = initial characteristics for forced convection

I. Introduction

THE number of publications on vaporization of fuel droplets is considerable.[1–9] These studies deal essentially with the vaporization of a pure liquid droplet, which is isolated[1–4] or placed with other droplets in evaporation.[5–9] Experiments take place in an enclosure at atmospheric pressure[6] or at high pressure[4] in natural convection (N.C), or in a thermal wind tunnel in forced convection (F.C). Other experiments take place in microgravity.[4] Models are based on the resolution of complete equations in the gaseous phase[3] or on the resolution of the conservation equations in gaseous films surrounding the droplet.[2,7] These equations are coupled to equations of heat transfer in the liquid phase.

Some studies concern the vaporization of binary mixture droplets in natural convection as well as in forced convection.[10–16] Confrontation of experiments undertaken in a thermal wind tunnel with a model of calculation in forced convection requires that the initial conditions of the experiment be taken into account because, during suspension of the droplet, vaporization takes place in natural convection. A recent work[16] concluded that in this case, analysis and qualification of experiments cannot take place if the calculation and the experiment

---

Received March 27, 1997; revision received Sept. 3, 1997; accepted for publication Sept. 10, 1997.

*Professor, Laboratoire de Mécanique Acoustique et Instrumentation (L.M.A.I. UPRES EA 1945), 52 Avenue de Villeneuve. E-mail: daif@univ-prep.fr.

†Graduate Student, L.M.A.I.

‡Assistant Professor, L.M.A.I.

are not associated during the natural convection phase. This approach is used in this work.

In this paper, we present the study of vaporization in forced convection of two or three binary fuel mixture droplets. Droplets situated one behind the other evaporate in the hot-airflow of a thermal wind tunnel equipped with a video recording system. During the suspension period of droplets, and before the opening of the obturator of the test section, the droplets partly evaporate in natural convection. The calculation model used to anticipate and qualify experiments is based on the concept of the gaseous films, sources of heat, and mass transfer in the gas. In the liquid, one solves equations of heat and mass transfer. In natural convection as well as in forced convection, the gaseous film thickness depends on the average Nusselt and Sherwood numbers, qualifying globally the heat and mass transfer around a wetted sphere in analogous conditions. These Nusselt and Sherwood numbers are expressed by correlations according to Grashof numbers[15,17] in the case of natural convection, and according to the Reynolds number[1] in the case of forced convection. To take into account the interaction of several droplets, one corrects correlations given by Renksizbulut et al.[1] by using expressions proposed by Chiang and Sirignano.[5] These expressions are extended to the cases of several constituents for the expression of Sherwood numbers.

II. Calculation Model

The model that we use is a generalization of the global model of Abramzon and Sirignano[2] and Daïf et al.[7,11] (Fig. 1). It processes the heat and mass conservation equations around one or several multicomponent droplets in evaporation in natural or forced convection. The resolution of these equations is based on the film theory, which supposes the existence of gaseous films (mass and thermal) around the droplet, limiting the integration area of these equations. These same equations are coupled to equations of heat and mass transfer in the liquid phase. To account for the fluid movement inside the droplet (Hills' vortex), the thermal diffusivity and mass diffusion coefficients are corrected.[13] The system of equations and the appropriate boundary conditions, as well as the method of resolution, are described in the literature.[2,7,10,14] The integration areas of the conservation equations are defined by their external radius.

For heat transfer, the external radius of the film depends on the Nusselt number,[2] and for a droplet i, its expression is

$$r_{fTi} = r_{is}\overline{Nu}_i/(\overline{Nu}_i - 2) \tag{1}$$

For each film mass caused by the j component of i, the external radius depends on the Sherwood number,[2] and is given by

$$r_{fMij} = r_{is}\overline{Sh}_{ij}/(\overline{Sh}_{ij} - 2) \tag{2}$$

As indicated in the Introduction, the average Nusselt and Sherwood numbers are expressed by correlations formed in natural convection as well as in forced convection. These Nusselt and Sherwood numbers are corrected to take into account the interaction for the case of several droplets.

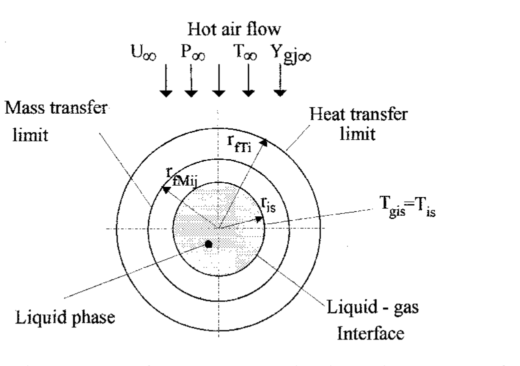

Fig. 1 Physical model of droplet vaporization with gaseous film.

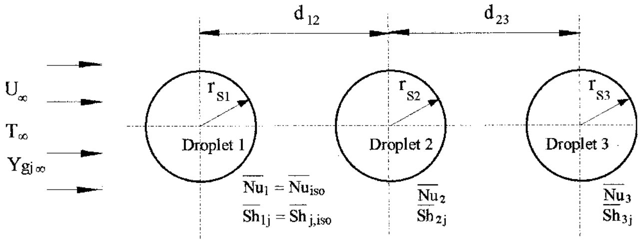

Fig. 2 Schematization of three droplets in evaporation in a test section of a thermal wind tunnel.

A. Correlations in Natural Convection

Expressions have been established by us for a pure hydrocarbon.[17] They are extended to a mixture of hydrocarbons.[15] These correlations are a function of G_m. To each i droplet considered we have

$$\overline{Nu}_i = 2 + 0.591(1 + B_{Ti})^{-0.588}Pr_i^{1/3}Gr_{mi}^{1/4} \tag{3}$$

with

$$10^{-3} \leq Gr_{mi} \leq 8.10^4$$

$$\overline{Sh}_{ij} = 2 + 0.574(1 + B_{Mi})^{0.089}Sc_{ij}^{1/3}Gr_{mi}^{1/4} \tag{4}$$

B. Correlations in Forced Convection

For an isolated droplet evaporating in a hot airflow, expressions of $\overline{Nu}_i$ and $\overline{Sh}_{ij}$ have been proposed[1] and are functions of Re_{mi}. They are written as

$$\overline{Nu}_{i,\mathrm{iso}} = (2 + 0,\ 57Re_{mi}^{1/2}Pr_i^{1/3})(1 + B_{Ti})^{-0,7} \tag{5}$$

with

$$10 \leq Re_{mi} \leq 300$$

$$\overline{Sh}_{ij,\mathrm{iso}} = (2 + 0,\ 87Re_{mi}^{1/2}Sc_{ij}^{1/3})(1 + B_{Mi})^{-0,7} \tag{6}$$

C. Interaction of Several Droplets in Forced Convection

As a recent work[7] has shown, only the evaporation in forced convection of a droplet positioned downstream of one or several droplets is modified. In the present work, we use only correlations[5] showing the influence of the first droplet on the second. The concept of the film is used by supposing that in the first approximation, the interaction is purely mechanical and caused essentially by the presence of the lead droplet, which masks the flow. This approximation is applied for several droplets (each droplet is influenced only by the one preceding it). At each calculation stage one solves the problem by processing the first droplet (isolated droplet), then the second according to the state of the first, then the third according to the state of the second, and so on, if necessary (Fig. 2).

Correlations[5] giving $\overline{Nu}$ and $\overline{Sh}$ for two droplets, according to these same numbers for isolated droplets, are a function of the distance between the centers of the droplets and the radius of the droplets. These correlations are extended to the case of several droplets and several constituents. For a droplet of i rank and a j constituent, they are written as

$$\frac{\overline{Nu}_i}{\overline{Nu}_{i,\mathrm{iso}}} = 0.528Re_{mi}^{-0.146}Pr_i^{-0.768}(1 + B_{Ti})^{0.356} \times \left[\frac{\mathrm{d}_{(i-1)i}}{r_{(i-1)0s}}\right]^{0.262}\left[\frac{r_{is}}{r_{(i-1)s}}\right]^{0.147} \tag{7}$$

$$\frac{\overline{Sh}_{ij}}{\overline{Sh}_{ij,\mathrm{iso}}} = 0.974 Re_{mi}^{0.127} Sc_{ij}^{-0.318} (1 + B_{Mi})^{-0.363} \times \left[\frac{d_{(i-1)i}}{r_{(i-1)0s}}\right]^{-0.064} \left[\frac{r_{is}}{r_{(i-1)s}}\right]^{0.857} \tag{8}$$

with

$0 \leq B_{Ti} \leq 2.52, \quad 0 \leq B_{Mi} \leq 1.27$

$11 \leq Re_{mi} \leq 254 \qquad 2 \leq i \leq n$ droplets

$0.68 \leq Pr_i \leq 0.91, \quad 1.48 \leq Sc_{ij} \leq 2.44$

III. Experimental Setup

The experimental setup (Fig. 3) allows us to study the evaporation of one or several droplets of fuel at atmospheric pressure. This setup includes a rectangular test section (50 × 70 mm) situated at the horizontal extremity of a thermal wind tunnel equipped with homogenization grids to make the flow uniform in the test section. Thermal protection ensures the insulation of the wind tunnel and thus limits the heat losses. In the test section the hot airflow, with average speed between 0 and 10 m s^{-1}, is generated by a centrifugal ventilator. The heating element (electrical resistance), controlled by a regulator, can maintain a maximum constant temperature of 150°C in the test section.

At the center of the test section, droplets are suspended on the extremities of glass capillaries 0.2–0.3 mm in diameter with three-point fixing. The central support remains fixed, and the micrometric movement of lateral supports allows us to adjust the initial distances between droplets. The observation of the phenomenon is rendered possible by an optical access on each face of the test section.

This setup is provided with a mechanical obturator situated at the entry of the test section. When the obturator is closed, the hot airflow is ejected from the circuit without passing the test section, which ensures establishment of a permanent speed and temperature level in the rest of the wind tunnel. The suspension of droplets on their support is then undertaken with a syringe in the test section at room temperature. When the obturator is open, the heated flow enters the test section and the forced convection sequence can begin. The temperature of the air is controlled by a thermocouple. The speed measurement is given by a pitot tube connected to a manometer.

Sequences of evaporation are recorded by a video system (8 mm camcorder–charge-coupled device with 470,000 pixels) equipped with a macrophotography lens. A computer process (image acquisition board and software) digitalizes and compresses, in real or differed time, the video sequences, with a maximum speed equal to 25 images per second. The spatial definition of an image after decompression is 320 × 240 pixels, or 320 columns × 240 lines. The number of digital images, i.e., the length of the sequence, depends simply on the memory capacity of the computer.

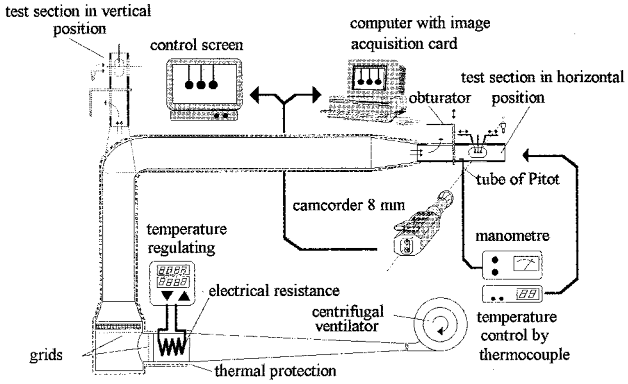

Fig. 3 Thermal wind tunnel and measuring instruments.

Droplets in evaporation are illuminated from the rear by a luminous base. This luminous base allows a strong contrast between the droplet and its support. The droplet will therefore appear to be opaque on the control screen and the base will appear to be rather white. This allows us to work directly on acquired images. These images are digitalized with an image acquisition board and present a high contrast in gray levels between the droplets and the base.

For an isolated droplet, the extraction of the contour is undertaken symmetrically on each side of the image. For a given line, one searches for the first somber pixel from the beginning of the line and from left to right (below a definite threshold level), corresponding to the left edge of the droplet, and for the first somber pixel from the end of the line and from right to left, corresponding to the right edge of the droplet. The operation is repeated for each line of the image. For each image, from contour of the droplet, we calculate the equivalent diameter of a sphere that would have the same volume. In the case of several droplets in evaporation, the same process is used several times, after a preliminary division of the image into vertical bands following the number of droplets studied.

IV. Results and Discussion

The results presented concern the evaporation of an isolated mixture droplet, two and three mixture droplets in interaction. Three initial compositions are examined: 50% heptane–50% decane, 2) 75% heptane–25% decane, and 3) 25% heptane–75% decane. The droplet diameters vary from 1 to 1.5 mm. Experimental conditions measured are, in cases 1 and 2, during the sequence in forced convection, $T_\infty = 348$ K and $U_\infty = 3.1$ m s^{-1}, and in case 3, during the sequence in forced convection, $T_\infty = 341$ K and $U_\infty = 3.36$ m s^{-1}.

A. Evaporation of an Isolated Droplet

Figure 4 represents the radius regression of a mixed droplet of 50% heptane–50% decane, as well as the calculated tem-

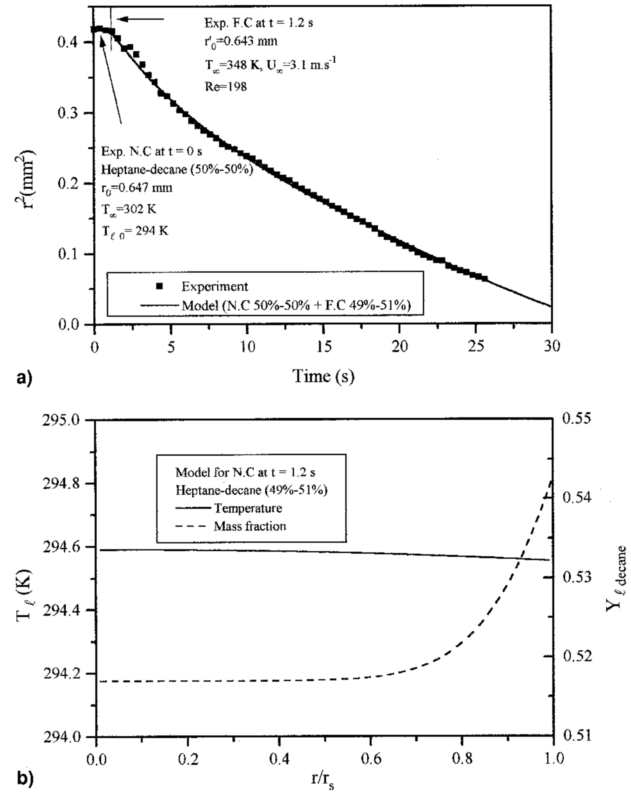

Fig. 4 Analysis of the vaporization sequence of an isolated mixture droplet (initial volumetric composition is 50% heptane–50% decane): a) time evolution of the radius, and b) temperatures and mass fraction profiles calculated inside the droplet at the end of N.C.

perature and mass fraction profiles inside the droplet at the end of the sequence, in natural convection. In Fig. 4a, one can observe that the model, in natural convection and in forced convection, confirms the experiment. The natural convection modifies the droplet temperature without any appreciable influence on radial distribution, and changes the mass fraction distribution of the decane, as also that of the heptane, from the center of the droplet to its surface (Fig. 4b). At the end of the sequence in natural convection, the average composition of the droplet is modified, and the new composition is then 49% heptane–51% decane (duration in natural convection is 1.2 s).

B. Evaporation in Interaction of Two Mixture Droplets

The same method of analysis used in the case of a single droplet is applied to the case of two droplets. Figure 5 shows the temporal evolution of the square of two radius droplets of 50% heptane–50% decane, as well as the distribution of temperature and mass fraction inside each of the droplets at the end of natural convection. Figure 5a shows a good agreement between the model and the experiment, despite vibrations undergone by the second droplet. These vibrations prevent the clarity of the images and falsify the analysis. In the distribution of temperature and mass fraction (Fig. 5b), the same phenomena that existed in the case of an isolated droplet are observed. At the end of the natural convection sequence, the average droplet composition is modified and passes from 50% heptane–50% decane to 45.3% heptane–54.7% decane for the first droplet (duration of natural convection is 10 s) and to 49% heptane–51% decane for the second droplet (duration of natural convection is 1.2 s).

Figure 6 shows a comparison between the experiment and calculation for droplet radius evolution of two mixture droplet systems in interaction (initial volumetric composition is 50% heptane–50% decane). Distances separating droplets vary from 1.68 to 1.93 mm. For two droplets having an initial composition of 75% heptane–25% decane, and for the distance $d_{1,2}$ equal to 3.1 mm, we compare results of the model to the experimental measures (Fig. 7). In Fig. 8 we present the study of two droplets whose initial composition is 25% heptane–75% decane, with $d_{1,2}$ equal to 3.69 mm.

Note that we do not measure the initial diameter of the droplets precisely; the first droplet can have a diameter greater than the second and vice versa. However, despite an experimental parameter variability (report of initial radius, Reynolds number, distances between droplets, initial composition), one observes with these three series of measurements considerable agreement between the model and experiment. The model predicts correctly the effect of the interaction of two droplets.

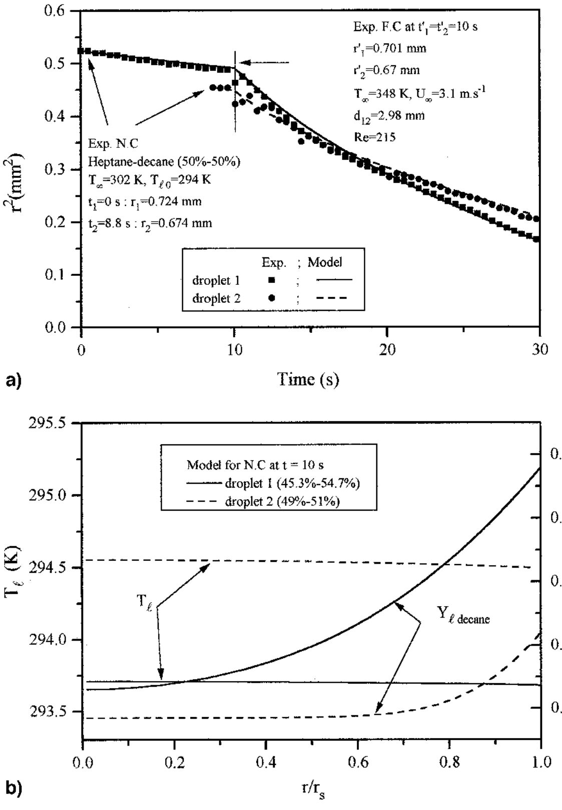

Fig. 5 Analysis of vaporization sequence of an interactive system of two mixture droplets (initial volumetric composition is 50% heptane–50% decane): a) time evolution of the radius, and b) temperatures and mass fraction profiles calculated inside the droplets at the end of N.C.

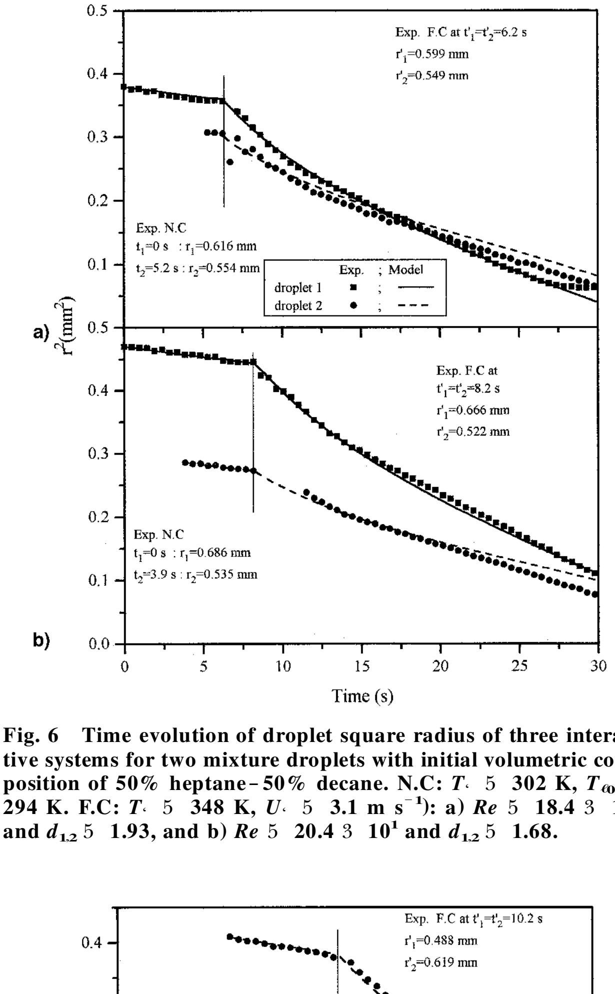

Fig. 6 Time evolution of droplet square radius of three interactive systems for two mixture droplets with initial volumetric composition of 50% heptane–50% decane. N.C: *T*‹ 5 302 K, $T_{\ell 0}$ 5 294 K. F.C: *T*‹ 5 348 K, *U*‹ 5 3.1 m s⁻¹): a) *Re* 5 18.4 3 10¹ and $d_{1,2}$ 5 1.93, and b) *Re* 5 20.4 3 10¹ and $d_{1,2}$ 5 1.68.

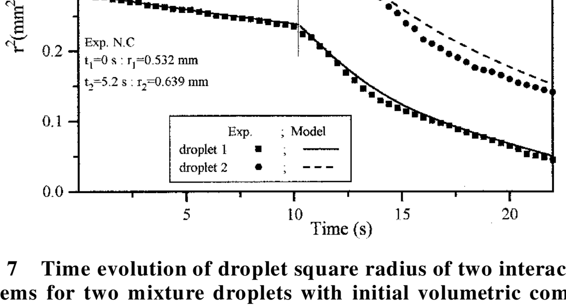

Fig. 7 Time evolution of droplet square radius of two interactive systems for two mixture droplets with initial volumetric composition of 75% heptane–25% decane. N.C: *T*‹ 5 302 K, $T_{\ell 0}$ 5 294 K. F.C: *T*‹ 5 348 K, *U*‹ 5 3.1 m s²¹. *Re* 5 1.50 3 10² and $d_{1,2}$ 5 3.1.

C. Evaporation in Interaction of Three Mixture Droplets

The method of analysis used in this case is the same as that used in the preceding cases. The example in Fig. 9 concerns the temporal evolution of the square radius of the three droplets (Fig. 9a), and the temperature and mass fraction profiles inside each droplet (Fig. 9b). In Fig. 9, one observes the same phenomena that were encountered in the preceding cases. The new composition at the end of the natural convection sequence is then 41.3% heptane–58.7% decane in the first droplet (duration of the natural convection is 14.4 s), 43.2% heptane–56.8% decane for the second droplet (duration of the natural convection is 11.4 s), and 47.8% heptane–52.2% decane for the third droplet (duration of the natural convection is 2.4 s).

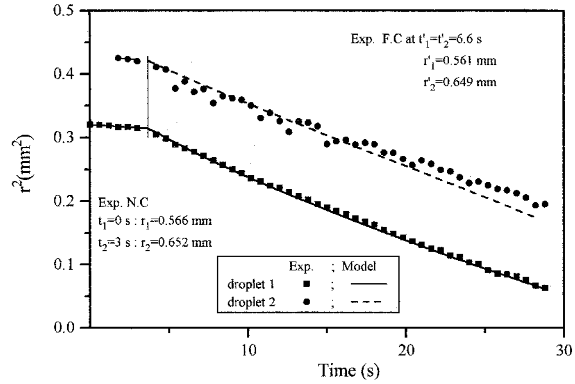

Fig. 8 Time evolution of droplet square radius of two interactive systems for two mixture droplets with initial volumetric composition of 25% heptane–75% decane. N.C: $T_`$ 5 300 K, $T_{\ell 0}$ 5 292 K. F.C: $T_`$ 5 341 K, $U_`$ 5 3.36 m s$^{2 1}$. *Re* 5 19.3 3 10^1 and $d_{1,2}$ 5 3.69.

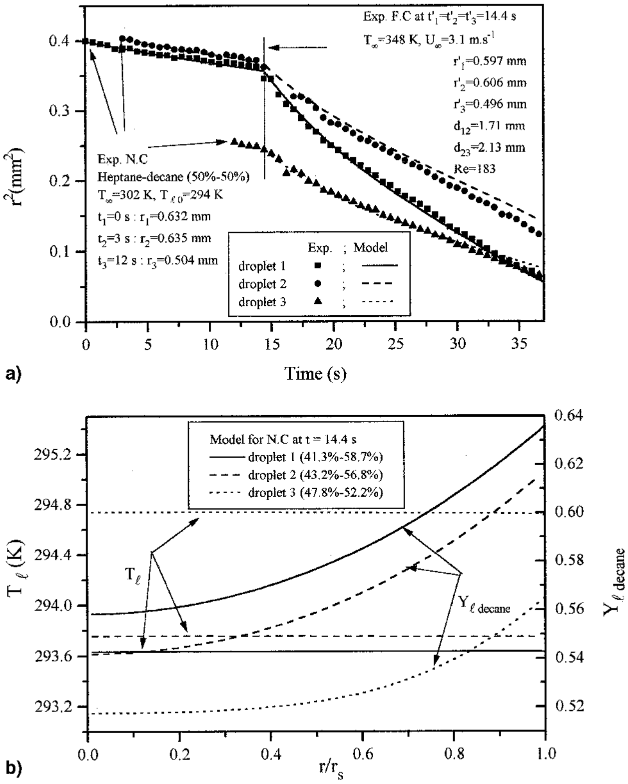

Fig. 9 Analysis of vaporization sequence of an interactive system of three mixture droplets (initial volumetric composition is 50% heptane–50% decane): a) time evolution of the radius; and b) temperatures and mass fraction profiles calculated inside the droplets at the end of N.C.

Figures 10–12 complete the study of three droplets in interaction. Three initial compositions are examined: 50% heptane–50% of decane (Fig. 10), 75% heptane–25% decane (Fig. 11), and 25% heptane–75% decane (Fig. 12). The distance separating the first two droplets varies between 1.96 and 2.37 mm, and $d_{2,3}$ falls between 1.58 and 2.2 mm. Similar to the case of two droplets, we do not obtain a precise droplet measurement. One observes from the whole of these figures that the effect of the interaction of the second on the third droplet is less significant than that of the first on the second. One can again note that the comparison between experimental and numerical results is satisfactory.

D. Parametric Study

This work is completed by a parametric study. It sets out to show the influence of the Reynolds number, the temperature of hot airflow, and the influence of the initial composition of

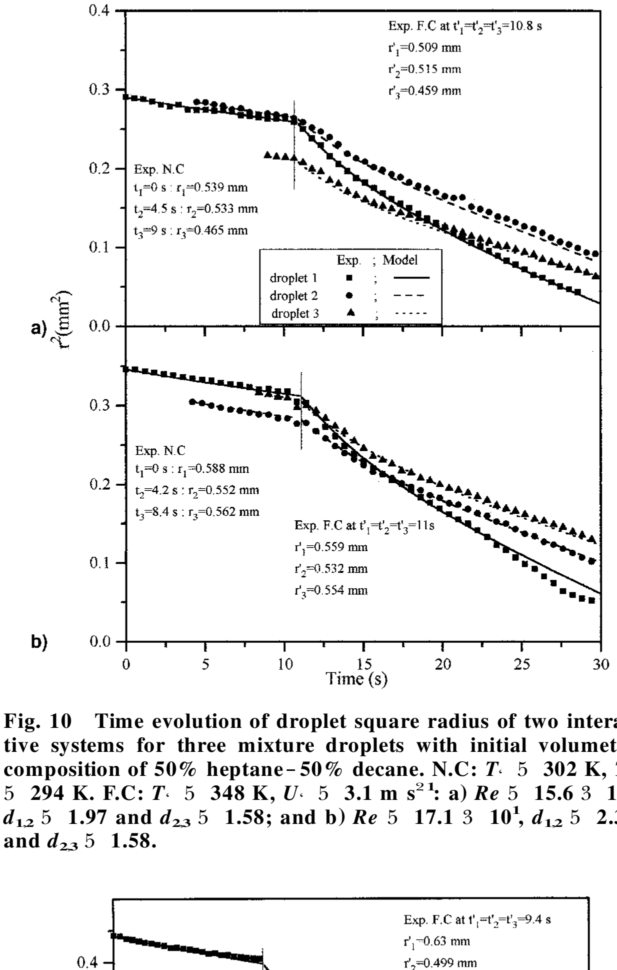

Fig. 10 Time evolution of droplet square radius of two interactive systems for three mixture droplets with initial volumetric composition of 50% heptane–50% decane. N.C: $T_`$ 5 302 K, $T_{\ell 0}$ 5 294 K. F.C: $T_`$ 5 348 K, $U_`$ 5 3.1 m s$^{2 1}$: a) *Re* 5 15.6 3 10^1, $d_{1,2}$ 5 1.97 and $d_{2,3}$ 5 1.58; and b) *Re* 5 17.1 3 10^1, $d_{1,2}$ 5 2.37, and $d_{2,3}$ 5 1.58.

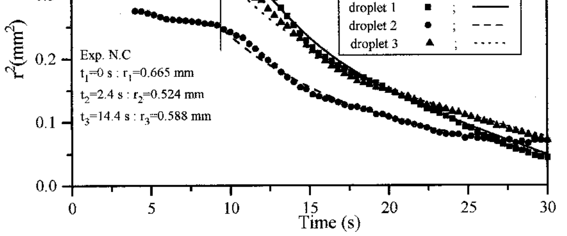

Fig. 11 Time evolution of droplet square radius of two interactive systems for three mixture droplets with initial volumetric composition of 75% heptane–25% decane. N.C: $T_`$ 5 302 K, $T_{\ell 0}$ 5 294 K. F.C: $T_`$ 5 348 K, $U_`$ 5 3.1 m s$^{2 1}$. *Re* 5 19.3 3 10^1, $d_{1,2}$ 5 2.06, and $d_{2,3}$ 5 1.59.

the mixture droplets on the vaporization in forced convection of two droplets in interaction. To do this, we define a K of each mixture droplet (downstream droplet) in interaction, as well as K_{iso} for an isolated mixture droplet (or lead droplet). For each study of the ratio K:K_{iso}, $d'_{1,2}$ is fixed, as are the thermophysical conditions. The proposed results concern forced convection, without a preliminary sequence in natural convection, and they are summarized in Fig. 13.

Figure 13a represents the influence of the Reynolds number. One can observe that the effect of the interaction increases with the Reynolds number, and more so when $d'_{1,2}$ is small.

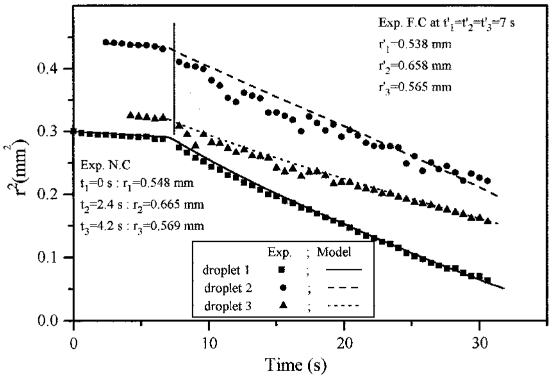

Fig. 12 Time evolution of droplet square radius of two interactive systems for three mixture droplets with initial volumetric composition of 25% heptane–75% decane. N.C: T‹ 5 300 K, T_{∞} 5 292 K. F.C: T‹ 5 341 K, U‹ 5 3.36 m s^{21}. Re 5 18.9 3 10^{1}, $d_{1,2}$ 5 1.96, and $d_{2,3}$ 5 2.2.

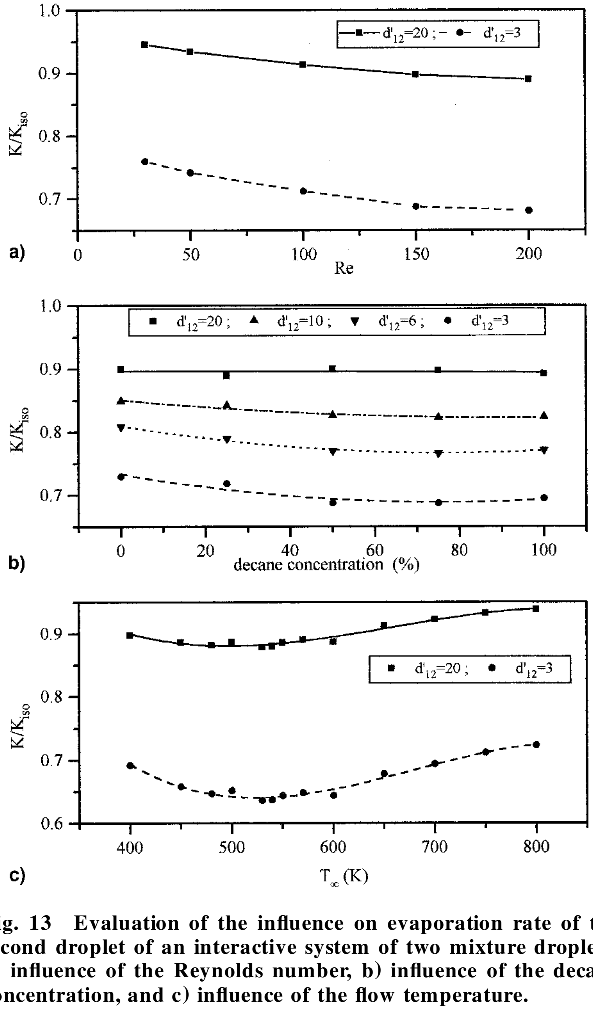

Fig. 13 Evaluation of the influence on evaporation rate of the second droplet of an interactive system of two mixture droplets: a) influence of the Reynolds number, b) influence of the decane concentration, and c) influence of the flow temperature.

For this simulation the initial composition of the mixture droplet is 50% heptane–50% decane. The hot airflow temperature is 400 K.

In Fig. 13b we present the influence of the composition of the mixture on the ratio K:K_{iso} for different distances between droplets and for $Re = 150$ and $T = 400$ K. The system of curves traced shows that the interaction is greater as the decane concentration increases (less volatile liquid). It is interesting to observe that the essential part of this increase takes place for a concentration of decane lower than 50%. Beyond this value, the supplementary effect is almost nil. The result is foreseeable when one observes the ratio K:K_{iso} for heptane or a pure decane droplet.

Figure 13c shows the influence of the gas temperature on the evaporation rate of droplets for two significant distances: 1) $d'_{1,2} = 3$, strong interaction, and 2) $d'_{1,2} = 20$, weak interaction. In this case, $Re = 1.5 \times 10^{2}$, and concentrations in the heptane and decane mixture are 50%. We observe that the interaction increases up to a value of T_{∞} close to the heptane T_{cr}, 540 K, and decreases when T_{∞} increases again. The secondary effect caused by the temperature is greater for smaller d'_{2}.

V. Conclusions

This work deals with a comparative experimental study calculating the evaporation in the interaction of two and three droplets of heptane and decane mixtures. The experiment, set up in a thermal wind tunnel, shows that evaporation of the mixture droplets occurs in two stages, the first in natural convection and the second in forced convection. The calculation model used is simple. It is based on the film theory. The thickness of the film, source of heat, and mass transfer always depend on the average Nusselt and Sherwood numbers characterizing these transfers. These Nusselt and Sherwood numbers are determined as a result of correlations that take into account the type of convection and the interaction in forced convection.

We described the analytical method concerning the evaporation of a mixture with an isolated droplet. This method is applied to the case of two and three mixture droplets in interaction: one observes that whatever the number of droplets, the average droplet composition at the end of the natural convection stage is appreciably different from the initial composition. Three series of experiments on two and three droplet evaporation of different initial composition mixtures and distances between droplets are compared with the numerical results. A considerably good agreement is shown to exist between the experiment and the calculation. When the distances are similar, the third droplet of the system actually undergoes a weak influence compared with the second droplet.

The numerical parametric study, undertaken in the case of two droplets, shows the growing influence of the initial volumetric fraction of decane on the interaction: Similarly, an increase of the dimensionless separation distance minimizes this effect. The effect of the interaction increases with the Reynolds number, regardless of the dimensionless separation distance. The influence of the flow temperature is greater when the dimensionless separation distance is lower. An increase in the temperature of the gas increases the interaction up to a limit that seems to depend on the most volatile constituent (hot airflow temperature is less than the critical temperature of heptane). After this characteristic temperature is passed, the secondary effect caused by the temperature inverts and the interaction decreases.

References

[1] Renksizbulut, M., Nafziger, R., and Li, X., "A Mass Transfer Correlation for Droplet Evaporation in High-Temperature Flows," *Chemical Engineering Science*, Vol. 46, No. 9, 1991, pp. 2351–2358.

[2] Abramzon, B., and Sirignano, W. A., "Droplet Vaporization Model for Spray Combustion Calculations," *International Journal of Heat and Mass Transfer*, Vol. 32, No. 9, 1989, pp. 1605–1618.

[3] Renksizbulut, M., and Haywood, J. A., "Transient Droplet Evaporation with Variable Properties and Internal Circulation at Intermediate Reynolds Numbers," *International Journal of Multiphase Flow*, Vol. 14, No. 2, 1988, pp. 189–202.

[4] Chauveau, C., Chesneau, X., and Gökalp, I., "High Pressure Vaporization and Burning of Methanol Droplets in Reduced Gravity," AIAA Paper 94-0430, Jan. 1994.

[5] Chiang, C. H., and Sirignano, W. A., "Interacting, Convection, Vaporizing Fuel Droplets with Variable Properties," *International Journal of Heat and Mass Transfer*, Vol. 36, No. 4, 1993, pp. 875–886.

[6] Bouaziz, M., Bresson, J., Chesneau, X., and Daïf, A., "Evaporation en Convection Naturelle de Gouttes de Combustibles en Forte Interaction," *Proceedings of the 16th Canadian Congress of Applied Mechanics*, Vol. 1, Univ. Laval, PQ, Canada, 1997, pp. 431, 432.

[7] Daïf, A., Bouaziz, M., Ali Chérif, A., Chesneau, X., and Bresson, J., "Modélisation et Expérimentation de la Vaporisation en Convection Forcée de Plusieurs Gouttes de Carburant en Interaction dans un Ecoulement d'Air Chauffé," *Entropie*, No. 201, 1996, pp. 19–27.

[8] Raju, M. S., and Sirignano, W. A., "Interaction Between Two Vaporizing Droplets in an Intermediate Reynolds Number Flow," *Physics of Fluids A*, Vol. 2, No. 10, 1990, pp. 1780–1796.

[9] Chiang, C. H., and Sirignano, W. A., "Axisymmetric Calculation of Three Droplet Interaction," *Atomization and Sprays*, Vol. 3, 1993, pp. 91–107.

[10] Ali Chérif, A., "Etude Théorique et Expérimentale de l'Evaporation de Gouttes à Plusieurs Constituants dans un Ecoulement d'Air Chauffé," Ph.D. Dissertation, Univ. de Perpignan, Perpignan, France, Dec. 1994.

[11] Daïf, A., Ali Chérif, A., Bresson, J., and Sarh, B., "Etude Numérique et Expérimentale de l'Evaporation d'une ou Plusieurs Gouttes de Mélange de Carburants dans un Ecoulement Chauffé," *Journal of Physics III*, Vol. 5, No. 10, 1995, pp. 1643–1660.

[12] Renksizbulut, M., and Bussmann, M., "Multicomponent Droplet Evaporation at Intermediate Reynolds Numbers," *International Journal of Heat and Mass Transfer*, Vol. 36, No. 11, 1993, pp. 2827–2835.

[13] Talley, D. G., and Yao, S. C., "A Semi Empirical Approach to Thermal and Composition Transients Inside Vaporizing Fuel Droplets," The Combustion Institute, Pittsburgh, PA, 1986, pp. 609–616.

[14] Continillo, G., and Sirignano, W. A., "Numerical Study of Multicomponent Fuel Spray Flame Propagation in a Spherical Closed Volume," *22nd Symposium (International) on Combustion*, The Combustion Institute, Pittsburgh, PA, 1988, pp. 1941–1949.

[15] Bouaziz, M., Daïf, A., Chesneau, X., and Ali Chérif, A., "Etude de la Vaporisation d'une Goutte de Mélanges de deux Carburants en Convection Naturelle," *Proceedings of the 1st Arab Mechanics Congress* (Damascus, Syria), Vol. 1, 1997, pp. 463–468.

[16] Bouaziz, M., Chesneau, X., Bresson, J., and Daïf, A., "Analysis of Experimental Study of Multicomponent Droplet Evaporation in Forced Convection," *Proceedings of the 2nd International Symposium on Contemporary Problems of Fluid Mechanics*, Yugoslav Society of Mechanics, Belgrade, Yugoslavia, 1996, pp. 237–240.

[17] Bouaziz, M., Daïf, A., Ali Chérif, A., and Chesneau, X., "Numerical Determination of the Correlations Qualifying the Mass and Heat Transfer Around a Sphere Saturated with a Pure Liquid in Natural Convection," *Book of Abstracts of the International Symposium on Advances in Computational Heat Transfer*, International Centre for Heat and Mass Transfer, Cesme, Turkey, June 1997, pp. 222–224.